

## Effects of spin–phonon interaction on the dynamical properties of thin ferroelectric films

This article has been downloaded from IOPscience. Please scroll down to see the full text article.

2005 J. Phys.: Condens. Matter 17 3001

(<http://iopscience.iop.org/0953-8984/17/19/014>)

View [the table of contents for this issue](#), or go to the [journal homepage](#) for more

Download details:

IP Address: 129.252.86.83

The article was downloaded on 28/05/2010 at 04:50

Please note that [terms and conditions apply](#).

# Effects of spin–phonon interaction on the dynamical properties of thin ferroelectric films

J M Wesselinowa

Department of Physics, University of Sofia, Boulevard J Bouchier 5, 1164 Sofia, Bulgaria

Received 14 January 2005, in final form 22 March 2005

Published 29 April 2005

Online at [stacks.iop.org/JPhysCM/17/3001](http://stacks.iop.org/JPhysCM/17/3001)

## Abstract

The effects of spin–phonon interaction on the temperature dependence of the spin-wave and phonon spectrum in thin ferroelectric transverse Ising films are studied using a Green function formalism beyond the random phase approximation. It is shown that due to the surface modes and the spin–phonon interaction the spin-wave damping effects in thin ferroelectric films are enhanced in comparison to the bulk. The phonon spectrum is discussed, too. Additional phonon damping and phonon frequency shift arise when the spin–phonon interaction is properly included.

## 1. Introduction

The surface and size effects on ferroelectric (FE) phase transitions have been extensively studied based on the Landau phenomenological theory [1–3]. Tilley and Zeks [3] studied in detail films with a second-order phase transition. Scott *et al* [1] and Wang *et al* [5] extended the studies to the first-order phase transition. On the microscopic level, the pseudo-spin theory based on the transverse Ising model (TIM) was also used to study the surface and size effects of FE phase transitions. Cottam *et al* [4] discussed the surface modes in semi-infinite FEs; Wang *et al* [6] and Sy [7] laid emphasis on the Curie temperature.

The phase behaviour of a thin FE film described by the TIM was recently investigated by Wang *et al* [8, 9] and Wesselinowa [10]. The dynamical properties of this model film were explored within the random-phase approximation (RPA) by Wang and Smith [11] ignoring the effects of damping. Using a Green function formalism Wesselinowa [12] calculated the temperature dependence of the soft modes of thin FE transverse Ising films including the effects of damping.

The structure and dielectric properties of FE thin films have been well investigated with different techniques; however, the lattice dynamics behaviour related to the ferroelectricity in thin films has not been completely understood. Recently, several research groups carried out Raman scattering studies to characterize the FE thin films and showed that all transverse optical (TO) phonons tended to depart from the corresponding positions of the bulk single crystal, implying that differences might exist between thin films and bulk single

crystals [13–18]. Using Raman spectroscopy the temperature dependence of the phonon modes for thin FE films of PbTiO<sub>3</sub> is discussed by Taguchi *et al* [16] and Fu *et al* [17]. It was shown that in comparison with the single crystal spectra, the Raman frequencies for the thin film shift remarkably to low frequencies and that the Raman lines are broad.

The aim of the present paper is to study the dynamical properties of a thin FE film including spin–phonon interactions using a Green function theory.

## 2. The model

In this section we present calculations for obtaining the damping effects from the Green function for a thin FE film including spin–phonon interactions. This is very important in order to explain the experimental data of Raman scattering lines from FE films, because the damping is related to the width of the half-maximum of the Raman scattering lines. The Hamiltonian of the pseudospin–phonon model of the film can be written as:

$$H = H_s + H_{\text{ph}} + H_{\text{sp}}. \quad (1)$$

$H_s$  is the Hamiltonian of the pseudospin system, i.e. the transverse Ising model:

$$H_s = -\Omega \sum_i S_i^x - \frac{1}{2} \sum_{ij} J_{ij} S_i^z S_j^z, \quad (2)$$

where  $S^x$  and  $S^z$  are components of spin- $\frac{1}{2}$  operators. The first term represents the tunnelling motion of the ions in one unit cell, while the second term describes the coupling between the quasi-spins belonging to different unit cells. We assume for simplicity only nearest-neighbour exchange interactions and take  $J_{ij} = J_s$ ;  $\Omega = \Omega_s$  on the surface layers ( $n = 1$  or  $N$ ) and  $J_{ij} = J_b$ ;  $\Omega = \Omega_b$  otherwise.

$H_{\text{ph}}$  contains the lattice vibrations including anharmonic phonon–phonon interactions:

$$H_{\text{ph}} = \frac{1}{2!} \sum_q (P_q P_{-q} + (\omega^0)^2 Q_q Q_{-q}) + \frac{1}{3!} \sum_{q, q_1} B(q, q_1) Q_q Q_{-q_1} Q_{q_1 - q} \\ + \frac{1}{4!} \sum_{q, q_1, q_2} A(q, q_1, q_2) Q_{q_1} Q_{q_2} Q_{-q - q_2} Q_{-q_1 + q}, \quad (3)$$

where  $Q_q$ ,  $P_q$  and  $\omega_q^0$  are the normal coordinate, momentum and frequency, respectively, of the lattice mode with a wavevector  $\mathbf{q}$ . The vibrational normal coordinate  $Q_q$  and the momentum  $P_q$  can be expressed in terms of phonon creation and annihilation operators:

$$Q_q = (2\omega_q^0)^{-1/2} (a_q + a_{-q}^+), \quad P_q = i(\omega_q^0/2)^{1/2} (a_q^+ - a_{-q}). \quad (4)$$

$H_{\text{sp}}$  describes the interaction of the pseudo-spins with the phonons:

$$H_{\text{sp}} = - \sum_q \bar{F}(q) Q_q S_{-q}^z - \frac{1}{2} \sum_{q, p} \bar{R}(q, p) Q_q Q_{-p} S_{p-q}^z + \text{h.c.}, \quad (5)$$

where the different terms denote spin–phonon interaction effects arising from the first, second, and third powers in the relative displacement of lattice site away from equilibrium.  $F(q) = \bar{F}(q)/(2\omega_q^0)^{1/2}$  and  $R(q, p) = \bar{R}(q, p)/(2\omega_q^0)^{1/2}(2\omega_p^0)^{1/2}$  designate the amplitudes for coupling phonons to the pseudo-spin-wave excitations in first, second, and third order, respectively.

In the ordered phase we have the mean values  $\langle S^x \rangle \neq 0$  and  $\langle S^z \rangle \neq 0$ , and it is appropriate to choose a new coordinate system rotating the original one used in (1) by the angle  $\theta$  in the  $xz$  plane [10]. The rotation angle  $\theta$  is determined by the requirement  $\langle S^{x'} \rangle = 0$  in the new coordinate system.

### 3. The transverse spin Green function

The retarded transverse spin Green function to be calculated is defined in matrix form as

$$G_{ij}(t) = \langle\langle B_i(t); B_j^\dagger(0) \rangle\rangle. \quad (6)$$

The operator  $B_{\mathbf{k}}$  stands symbolically for the set  $S_{\mathbf{k}}^+$ ,  $S_{-\mathbf{k}}^-$ . On introducing the two-dimensional Fourier transform  $G_{n_i n_j}(\mathbf{k}_{\parallel}, E)$ , one has the following form:

$$G_s^{+-} = \langle\langle S_i^+; S_j^- \rangle\rangle_E = \frac{\sigma}{N'} \sum_{\mathbf{k}_{\parallel}} \exp(i\mathbf{k}_{\parallel}(\mathbf{r}_i - \mathbf{r}_j)) G_{n_i n_j}(\mathbf{k}_{\parallel}, E), \quad (7)$$

where  $N'$  is the number of sites in any of the lattice planes.  $\sigma(T) = 2\langle S^z \rangle$  is the relative polarization in the direction of the mean field.  $\mathbf{r}_i$  represents the position vectors of site  $i$ ,  $n$  (or  $m$ ) = 1, ...,  $N$  denotes the layer ordering number beginning with one surface ( $n = 1$ ) and terminating with the other surface ( $n = N$ ).  $\mathbf{k}_{\parallel} = (k_x, k_y)$  is a two-dimensional wavevector parallel to the surface. The summation is taken over the Brillouin zone.

We assume for simplicity only nearest-neighbour exchange interactions and write all interaction constants for the surface layers ( $n = 1, N$ ) with index 's' and all others with index 'b'. For the approximate calculation of the Green function (7) we use a method proposed by Tserkovnikov [22], which is appropriate for spin problems. It goes beyond the random phase approximation (RPA) taking into account the correlation functions  $\bar{n}(\mathbf{k}_{\parallel})$  and  $\bar{N}(\mathbf{k}_{\parallel})$ , and the damping effects. Using the equation of motion beyond the RPA taking into account the coupling between the transverse pseudo-spin and the phonon modes we find that the Fourier-transformed Green function for an FE thin film, defined by equation (7), obeys for  $T \leq T_C$  the following  $2N \times 2N$  matrix form:

$$\begin{pmatrix} \mathbf{H}_-(E) & -\mathbf{Q} \\ \mathbf{Q} & \mathbf{H}_+(E) \end{pmatrix} \begin{pmatrix} \mathbf{G}_s^{+-} \\ \mathbf{G}_s^{+} \end{pmatrix} = \begin{pmatrix} \sigma \\ -\sigma \end{pmatrix}. \quad (8)$$

In that equation the quantities  $\mathbf{H}$  and  $\mathbf{Q}$  are  $N \times N$  matrices.  $\mathbf{H}_{\mp}(E)$  is given by:

$$\mathbf{H}_{\mp} = \begin{pmatrix} E \mp (v_1 - i\gamma_1^s) & k_1 & 0 & 0 & 0 & 0 & \dots \\ k_2 & E \mp (v_2 - i\gamma_2^s) & k_2 & 0 & 0 & 0 & \dots \\ 0 & k_3 & E \mp (v_3 - i\gamma_3^s) & k_3 & 0 & 0 & \dots \\ \vdots & \vdots & \vdots & \vdots & \vdots & \vdots & \ddots \\ 0 & 0 & 0 & 0 & 0 & k_N & E \mp (v_N - i\gamma_N^s) \end{pmatrix} \quad (9)$$

with

$$k_n = J_b^{\text{eff}} \sigma_n \sin^2 \theta_n, \quad n = 1, \dots, N,$$

$$\begin{aligned} v_n = & 2\Omega_n \sin \theta_n + \frac{1}{2} \sigma_n J_n^{\text{eff}} \cos^2 \theta_n - \frac{\sigma_n J_n^{\text{eff}}}{4} \sin^2 \theta_n \gamma(\mathbf{k}_{\parallel}) + J_{n-1}^{\text{eff}} \sigma_{n-1} \cos^2 \theta_{n-1} \\ & + J_{n+1}^{\text{eff}} \sigma_{n+1} \cos^2 \theta_{n+1} - \frac{J_n^{\text{eff}}}{N\sigma_n} \sum_{\mathbf{q}_{\parallel}} \left( \gamma(\mathbf{q}_{\parallel}) \cos^2 \theta_n \right. \\ & \left. - 0.5\gamma(\mathbf{k}_{\parallel} - \mathbf{q}_{\parallel}) \sin^2 \theta_n \right) \bar{n}_n(\mathbf{q}_{\parallel}) - \frac{J_{n-1}^{\text{eff}}}{N\sigma_{n-1}} \sum_{\mathbf{q}_{\parallel}} \gamma(\mathbf{q}_{\parallel}) \cos^2 \theta_{n-1} \bar{n}_{n-1}(\mathbf{q}_{\parallel}) \\ & - \frac{J_{n+1}^{\text{eff}}}{N\sigma_{n+1}} \sum_{\mathbf{q}_{\parallel}} \gamma(\mathbf{q}_{\parallel}) \cos^2 \theta_{n+1} \bar{n}_{n+1}(\mathbf{q}_{\parallel}), \end{aligned}$$

$$\gamma_n^s = \gamma_n^{\text{ss}} + \gamma_n^{\text{sp}},$$

$$\gamma_n^{\text{ss}} = \frac{\pi}{2N^2} \sum_{\mathbf{p}_{\parallel}, \mathbf{q}_{\parallel}} \left[ (V_n(\mathbf{q}_{\parallel}, \mathbf{k}_{\parallel} - \mathbf{q}_{\parallel}) + V_n(\mathbf{k}_{\parallel} - \mathbf{p}_{\parallel} - \mathbf{q}_{\parallel}, \mathbf{p}_{\parallel} + \mathbf{q}_{\parallel}))^2 \right]$$

$$\begin{aligned}
& \times [\bar{n}_n(\mathbf{p}_\parallel)(\sigma_n + \bar{n}_n(\mathbf{p}_\parallel + \mathbf{q}_\parallel) + \bar{n}_n(\mathbf{k}_\parallel - \mathbf{q}_\parallel)) - \bar{n}_n(\mathbf{p}_\parallel + \mathbf{q}_\parallel)\bar{n}_n(\mathbf{k}_\parallel - \mathbf{q}_\parallel)] \\
& \times \delta(\epsilon_n(\mathbf{k}_\parallel - \mathbf{q}_\parallel) + \epsilon_n(\mathbf{p}_\parallel + \mathbf{q}_\parallel) - \epsilon_n(\mathbf{p}_\parallel) - \epsilon_n(\mathbf{k}_\parallel)) \\
& + [(J_{n-1}^{\text{eff}}\gamma(\mathbf{q}_\parallel)\cos^2\theta_{n-1})^2 + (J_{n-1}^{\text{eff}}\gamma(\mathbf{k}_\parallel - \mathbf{p}_\parallel - \mathbf{q}_\parallel)\cos^2\theta_{n-1})^2] \\
& \times [\bar{n}_{n-1}(\mathbf{p}_\parallel)(\sigma_{n-1} + \bar{n}_{n-1}(\mathbf{p}_\parallel + \mathbf{q}_\parallel) + \bar{n}_{n-1}(\mathbf{k}_\parallel - \mathbf{q}_\parallel)) \\
& - \bar{n}_{n-1}(\mathbf{p}_\parallel + \mathbf{q}_\parallel)\bar{n}_{n-1}(\mathbf{k}_\parallel - \mathbf{q}_\parallel)] \\
& \times \delta(\epsilon_{n-1}(\mathbf{k}_\parallel - \mathbf{q}_\parallel) + \epsilon_{n-1}(\mathbf{p}_\parallel + \mathbf{q}_\parallel) - \epsilon_{n-1}(\mathbf{p}_\parallel) - \epsilon_{n-1}(\mathbf{k}_\parallel)) \\
& + [(J_{n+1}^{\text{eff}}\gamma(\mathbf{q}_\parallel)\cos^2\theta_{n+1})^2 + (J_{n+1}^{\text{eff}}\gamma(\mathbf{k}_\parallel - \mathbf{p}_\parallel - \mathbf{q}_\parallel)\cos^2\theta_{n+1})^2] \\
& \times [\bar{n}_{n+1}(\mathbf{p}_\parallel)(\sigma_{n+1} + \bar{n}_{n+1}(\mathbf{p}_\parallel + \mathbf{q}_\parallel) + \bar{n}_{n+1}(\mathbf{k}_\parallel - \mathbf{q}_\parallel)) \\
& - \bar{n}_{n+1}(\mathbf{p}_\parallel + \mathbf{q}_\parallel)\bar{n}_{n+1}(\mathbf{k}_\parallel - \mathbf{q}_\parallel)] \\
& \times \delta(\epsilon_{n+1}(\mathbf{k}_\parallel - \mathbf{q}_\parallel) + \epsilon_{n+1}(\mathbf{p}_\parallel + \mathbf{q}_\parallel) - \epsilon_{n+1}(\mathbf{p}_\parallel) - \epsilon_{n+1}(\mathbf{k}_\parallel)) \Big], \\
\gamma_n^{\text{sp}} = & \frac{\pi \sin^2\theta_n}{4} F_n^2(\mathbf{k}_\parallel)\delta(\bar{\omega}_n(\mathbf{k}_\parallel) - \epsilon_n(\mathbf{k}_\parallel)) + \frac{\pi \cos^2\theta_n}{N} \sum_{\mathbf{q}_\parallel} F_n^2(\mathbf{q}_\parallel) \\
& \times [(\bar{N}_n(\mathbf{q}_\parallel) - \bar{n}_n(\mathbf{k}_\parallel - \mathbf{q}_\parallel))\delta(-\bar{\omega}_n(\mathbf{q}_\parallel) + \epsilon_n(\mathbf{k}_\parallel - \mathbf{q}_\parallel) - \epsilon_n(\mathbf{k}_\parallel)) \\
& + (1 + \bar{N}_n(\mathbf{q}_\parallel) + \bar{n}_n(\mathbf{k}_\parallel - \mathbf{q}_\parallel))\delta(\bar{\omega}_n(\mathbf{q}_\parallel) + \epsilon_n(\mathbf{k}_\parallel - \mathbf{q}_\parallel) - \epsilon_n(\mathbf{k}_\parallel))] \\
& + \frac{\pi \cos^2\theta_n}{2N^2} \sum_{\mathbf{q}_\parallel, \mathbf{p}_\parallel} R_n^2(\mathbf{q}_\parallel, \mathbf{p}_\parallel)[\bar{N}_n(\mathbf{p}_\parallel)(1 + \bar{N}_n(\mathbf{q}_\parallel) + \bar{n}_n(\mathbf{k}_\parallel + \mathbf{p}_\parallel - \mathbf{q}_\parallel)) \\
& - \bar{N}_n(\mathbf{q}_\parallel)\bar{n}_n(\mathbf{k}_\parallel + \mathbf{p}_\parallel - \mathbf{q}_\parallel)]\delta(\bar{\omega}_n(\mathbf{q}_\parallel) - \bar{\omega}_n(\mathbf{p}_\parallel) + \epsilon_n(\mathbf{k}_\parallel + \mathbf{p}_\parallel - \mathbf{q}_\parallel) - \epsilon_n(\mathbf{k}_\parallel)) \\
& + \frac{\pi \sin^2\theta_n}{8N} \sum_{\mathbf{q}_\parallel} R_n^2(\mathbf{q}_\parallel, \mathbf{k}_\parallel + \mathbf{q}_\parallel)(\bar{N}_n(\mathbf{q}_\parallel) - \bar{N}_n(\mathbf{k}_\parallel + \mathbf{q}_\parallel)) \\
& \times \delta(\bar{\omega}_n(\mathbf{k}_\parallel + \mathbf{q}_\parallel) + \bar{\omega}_n(\mathbf{q}_\parallel) - \epsilon_n(\mathbf{k}_\parallel)), \\
\gamma(\mathbf{k}_\parallel) = & \frac{1}{2}(\cos(k_x a) + \cos(k_y a)), \\
\bar{n}_n(\mathbf{q}_\parallel) = & \langle S_{\mathbf{q}_\parallel}^- S_{\mathbf{q}_\parallel}^+ \rangle_n, \quad \bar{N}_n(\mathbf{q}_\parallel) = \langle a_{\mathbf{q}_\parallel}^+ a_{\mathbf{q}_\parallel}^- \rangle_n, \\
V_n(\mathbf{q}_\parallel, \mathbf{k}_\parallel - \mathbf{q}_\parallel) = & J_n^{\text{eff}}(\cos^2\theta_n\gamma(\mathbf{q}_\parallel) - 0.5\sin^2\theta_n\gamma(\mathbf{k}_\parallel - \mathbf{q}_\parallel)).
\end{aligned}$$

The pseudo-spin–phonon interaction causes a renormalization of the spin–spin–interaction constant  $J \rightarrow J_{\text{eff}}$  with  $J_{\text{eff}}$ :

$$J_{\text{eff}} = J_0 + \frac{2F_0 F_k \delta_{k0}}{\omega_k - \sigma \cos\theta R_k + 0.5A_k}, \quad (10)$$

which is now temperature dependent. The anharmonicity phonon–phonon parameter  $A(\mathbf{k}_\parallel)$  and the second spin–phonon parameter  $R(\mathbf{k}_\parallel)$  will decrease the effective exchange coupling  $J_{\text{eff}}$ , while the first pseudo-spin–lattice constant  $F(\mathbf{k}_\parallel)$  will increase its value.  $\epsilon_n(\mathbf{k}_\parallel) = \sqrt{(\epsilon_n^{11})^2 - (\epsilon_n^{12})^2}$  is the renormalized transverse pseudo-spin energy,  $\gamma_n^{11}(\mathbf{k}_\parallel)$  is the transverse spin-wave damping of the  $n$ th layer and  $\bar{\omega}_n(\mathbf{k}_\parallel)$  is the renormalized optic phonon energy obtained in section 4. Here we have introduced the notations  $J_1 = J_N = J_s$ ,  $J_n = J_b$  ( $n = 2, 3, 4, \dots, N-1$ ),  $\Omega_1 = \Omega_N = \Omega_s$ ,  $\Omega_n = \Omega_b$  ( $n = 2, 3, 4, \dots, N-1$ ),  $J_0 = J_{N+1} = 0$ . Analogous notations are used to describe all interaction parameters of the model. The other

quantity  $\mathbf{Q}$  is given by the following expression:

$$\mathbf{Q} = \begin{pmatrix} d_1 & k_1 & 0 & 0 & 0 & 0 & \dots \\ k_2 & d_2 & k_2 & 0 & 0 & 0 & \dots \\ 0 & k_3 & d_3 & k_3 & 0 & 0 & \dots \\ \vdots & \vdots & \vdots & \vdots & \vdots & \vdots & \ddots \\ 0 & 0 & 0 & 0 & 0 & k_N & d_N \end{pmatrix} \quad (11)$$

with

$$k_n = J_b^{\text{eff}} \sigma_n \sin^2 \theta_n, \quad n = 1, \dots, N,$$

$$d_n = -\frac{\sigma_n J_n^{\text{eff}}}{4} \sin^2 \theta_n \gamma(\mathbf{k}_{\parallel}).$$

For the rotation angle  $\theta$  we have the following two solutions in the generalized Hartree–Fock approximation:

1.  $\cos \theta = 0$ , i.e.  $\theta = \frac{\pi}{2}$ , if  $T \geq T_C$ ;
2.  $\sin \theta = \frac{4\Omega}{\sigma J^{\text{eff}}} = \frac{\sigma_c}{\sigma}$ , if  $T \leq T_C$ .

In order to obtain the solutions of the matrix equation (6), we define two-dimensional column matrices,  $\mathbf{G}_m$  and  $\mathbf{R}_m$ , with the elements given by  $(\mathbf{G}_n)_m = G_{mn}$  and  $(\mathbf{R}_n)_m = \sigma_n \delta_{mn}$ , so that equation (7) yields:

$$\mathbf{H}(E)\mathbf{G}_n = \mathbf{R}_n. \quad (12)$$

From equation (12),  $G_{nn}(E)$  is obtained as:

$$G_{nn}(E) = \frac{|H_{nn}(E)|}{|H(E)|}, \quad (13)$$

where  $|H_{nn}(E)|$  is the determinant made by replacing the  $n$ th column of the determinant  $|H(E)|$  by  $R_n$ . The poles of the Green function  $G_{nn}(E)$  can be obtained by solving  $|H(E)| = 0$ .

#### 4. The phonon Green function

For the retarded phonon Green function we have the matrix:

$$\bar{G}_{ij}(t) = \langle \langle \bar{B}_i(t); \bar{B}_j^+(0) \rangle \rangle. \quad (14)$$

The operator  $\bar{B}_{\mathbf{k}}$  stands symbolically for the set of phonon annihilation and creation operators  $a_{\mathbf{k}}, a_{-\mathbf{k}}^+$ . Analogously to the calculation of the spin Green function in the previous section using the method of Tserkovnikov [22], we obtain for the equation of motion for a ferroelectric thin film for  $T \leq T_C$  beyond the RPA the following  $2N \times 2N$  matrix form:

$$\begin{pmatrix} \mathbf{M}_-(E) & -\mathbf{S} \\ \mathbf{S} & \mathbf{M}_+(E) \end{pmatrix} \begin{pmatrix} \mathbf{G}_{\text{ph}}^{-+} \\ \mathbf{G}_{\text{ph}}^{+-} \end{pmatrix} = \begin{pmatrix} 1 \\ -1 \end{pmatrix}. \quad (15)$$

The quantities  $\bar{M}$  and  $\bar{S}$  are  $N \times N$  matrices.  $\bar{M}_{\mp}(E)$  is given by:

$$\mathbf{M}_{\mp} = \begin{pmatrix} E \mp (w_1 - i\Gamma_1^{\text{ph}}) & K_1 & 0 & 0 & 0 & 0 & \dots \\ K_2 & E \mp (w_2 - i\Gamma_2^{\text{ph}}) & K_2 & 0 & 0 & 0 & \dots \\ 0 & K_3 & E \mp (w_3 - i\Gamma_3^{\text{ph}}) & K_3 & 0 & 0 & \dots \\ \vdots & \vdots & \vdots & \vdots & \vdots & \vdots & \ddots \\ 0 & 0 & 0 & 0 & 0 & K_N & E \mp (w_N - i\Gamma_N^{\text{ph}}) \end{pmatrix} \quad (16)$$

where

$$K_n = 2\sigma_n \cos \theta_n R_n,$$

$$w_n = \omega^0(\mathbf{k}_{\parallel}) + B_n(\mathbf{k}_{\parallel}) \langle \mathcal{Q}_n(\mathbf{k}_{\parallel}) \rangle \delta_{\mathbf{k}_{\parallel}0} + 0.5 \sum_{\mathbf{q}_{\parallel}} A_n(\mathbf{k}_{\parallel} \mathbf{q}_{\parallel}) (2\bar{N}_n(\mathbf{q}_{\parallel}) + 1) - 0.5\sigma_n \cos \theta_n R_n(\mathbf{k}_{\parallel}),$$

$$\Gamma_n^{\text{ph}} = \Gamma_n^{\text{ph-ph}} + \Gamma_n^{\text{sp-ph}},$$

$$\begin{aligned} \Gamma_n^{\text{ph-ph}} = & \frac{9\pi}{N'} \sum_{\mathbf{q}_{\parallel}} B_n^2(\mathbf{k}_{\parallel}, \mathbf{q}_{\parallel}) (\bar{N}_n(\mathbf{q}_{\parallel}) - \bar{N}_n(\mathbf{k}_{\parallel} - \mathbf{q}_{\parallel})) \\ & \times [\delta(\bar{\omega}_n(\mathbf{q}_{\parallel}) - \bar{\omega}_n(\mathbf{k}_{\parallel} - \mathbf{q}_{\parallel}) - \bar{\omega}_n(\mathbf{k}_{\parallel})) - \delta(\bar{\omega}_n(\mathbf{k}_{\parallel} - \mathbf{q}_{\parallel}) - \bar{\omega}_n(\mathbf{q}_{\parallel}) - \bar{\omega}_n(\mathbf{k}_{\parallel}))] \\ & + \frac{16\pi}{N'^2} \sum_{\mathbf{q}_{\parallel}, \mathbf{p}_{\parallel}} A_n^2(\mathbf{k}_{\parallel}, \mathbf{q}_{\parallel}, \mathbf{p}_{\parallel}) [\bar{N}_n(\mathbf{p}_{\parallel}) (1 + \bar{N}_n(\mathbf{q}_{\parallel}) + \bar{N}_n(\mathbf{p}_{\parallel} + \mathbf{k}_{\parallel} - \mathbf{q}_{\parallel})) \\ & - \bar{N}_n(\mathbf{q}_{\parallel}) \bar{N}_n(\mathbf{p}_{\parallel} + \mathbf{k}_{\parallel} - \mathbf{q}_{\parallel})] \\ & \times \delta(\bar{\omega}_n(\mathbf{q}_{\parallel}) + \bar{\omega}_n(\mathbf{p}_{\parallel} + \mathbf{k}_{\parallel} - \mathbf{q}_{\parallel}) - \bar{\omega}_n(\mathbf{p}_{\parallel}) - \bar{\omega}_n(\mathbf{k}_{\parallel})), \end{aligned}$$

$$\begin{aligned} \Gamma_n^{\text{sp-ph}} = & \frac{\pi \sigma_n \sin^2 \theta_n}{4} F_n^2(\mathbf{k}_{\parallel}) \delta(\epsilon_n(\mathbf{k}_{\parallel}) - \bar{\omega}_n(\mathbf{k}_{\parallel})) \\ & + \frac{\pi \sigma_n \cos^2 \theta_n}{N'^2} \sum_{\mathbf{q}_{\parallel}, \mathbf{p}_{\parallel}} R_n^2(\mathbf{k}_{\parallel}, \mathbf{q}_{\parallel}) [\bar{n}_n(\mathbf{p}_{\parallel}) (1 + \bar{N}_n(\mathbf{q}_{\parallel}) + \bar{n}_n(\mathbf{p}_{\parallel} + \mathbf{k}_{\parallel} - \mathbf{q}_{\parallel})) \\ & - \bar{N}_n(\mathbf{q}_{\parallel}) \bar{n}_n(\mathbf{p}_{\parallel} + \mathbf{k}_{\parallel} - \mathbf{q}_{\parallel})] \\ & \times \delta(\bar{\omega}_n(\mathbf{q}_{\parallel}) + \epsilon_n(\mathbf{p}_{\parallel} + \mathbf{k}_{\parallel} - \mathbf{q}_{\parallel}) - \epsilon_n(\mathbf{p}_{\parallel}) - \bar{\omega}_n(\mathbf{k}_{\parallel})) \\ & + \frac{\pi \sigma_n \sin^2 \theta_n}{4N'} \sum_{\mathbf{q}_{\parallel}} R_n^2(\mathbf{k}_{\parallel}, \mathbf{q}_{\parallel}) [(\bar{N}_n(\mathbf{q}_{\parallel}) - \bar{n}_n(\mathbf{k}_{\parallel} - \mathbf{q}_{\parallel})) \\ & \times \delta(\bar{\omega}_n(\mathbf{q}_{\parallel}) - \epsilon_n(\mathbf{k}_{\parallel} - \mathbf{q}_{\parallel}) - \bar{\omega}_n(\mathbf{k}_{\parallel})) + (1 + \bar{N}_n(\mathbf{q}_{\parallel}) + \bar{n}_n(\mathbf{k}_{\parallel} - \mathbf{q}_{\parallel})) \\ & \times \delta(\bar{\omega}_n(\mathbf{q}_{\parallel}) + \epsilon_n(\mathbf{p}_{\parallel} + \mathbf{k}_{\parallel} - \mathbf{q}_{\parallel}) + \epsilon_n(\mathbf{p}_{\parallel}) - \bar{\omega}_n(\mathbf{k}_{\parallel}))], \end{aligned}$$

with

$$\begin{aligned} \langle \mathcal{Q}_n(\mathbf{k}_{\parallel}) \rangle = & \left( 0.5\sigma_n^2 \cos^2 \theta_n F_n(\mathbf{k}_{\parallel}) - \frac{1}{N'} \sum_{\mathbf{q}_{\parallel}} B_n(\mathbf{k}_{\parallel} \mathbf{q}_{\parallel}) (2\bar{N}_n(\mathbf{q}_{\parallel}) + 1) \right) \\ & \times \left( \omega_n(\mathbf{k}_{\parallel}) - 0.5\sigma_n^2 \cos^2 \theta_n R_n(\mathbf{k}_{\parallel}) + \frac{1}{N'} \sum_{\mathbf{q}_{\parallel}} A_n(\mathbf{k}_{\parallel} \mathbf{q}_{\parallel}) (2\bar{N}_n(\mathbf{q}_{\parallel}) + 1) \right)^{-1}. \end{aligned}$$

The other quantity  $\mathbf{S}$  is given by the following expression:

$$\mathbf{S} = \begin{pmatrix} T_1 & K_1 & 0 & 0 & 0 & 0 & \dots \\ K_2 & T_2 & K_2 & 0 & 0 & 0 & \dots \\ 0 & K_3 & T_3 & K_3 & 0 & 0 & \dots \\ \vdots & \vdots & \vdots & \vdots & \vdots & \vdots & \ddots \\ 0 & 0 & 0 & 0 & 0 & K_N & T_N \end{pmatrix} \quad (17)$$

with

$$K_n = 2\sigma_n \cos \theta_n R_n,$$

$$T_n = w_n(\mathbf{k}_{\parallel}) - \omega^0(\mathbf{k}_{\parallel}).$$

The phonon energy  $\omega^0(\mathbf{k}_{\parallel})$  is renormalized due to the anharmonic phonon interaction terms:

$$\begin{aligned} \bar{\omega}_n^2 = & (\omega^0)^2(\mathbf{k}_{\parallel}) - 2\omega^0(\mathbf{k}_{\parallel}) \left( \frac{\sigma_n^2 \cos^2 \theta_n}{4} R_n(\mathbf{k}_{\parallel}) + \frac{\sin^2 \theta_n}{4N'} \sum_{\mathbf{q}_{\parallel}} R_n(\mathbf{k}_{\parallel} \mathbf{q}_{\parallel}) \bar{n}_n(\mathbf{q}_{\parallel}) \right. \\ & \left. - \frac{1}{2N'} \sum_{\mathbf{q}_{\parallel}} A_n(\mathbf{k}_{\parallel} \mathbf{q}_{\parallel}) (2\bar{N}_n(\mathbf{q}_{\parallel}) + 1) - B_n(\mathbf{k}_{\parallel}) (Q_n(\mathbf{k}_{\parallel})) \delta_{\mathbf{k}_{\parallel}0} \right). \end{aligned} \quad (18)$$

If they are not taken into account, then  $\bar{\omega}(\mathbf{k}_{\parallel})$  is identical with the energy of the uncoupled phonon  $\omega^0(\mathbf{k}_{\parallel})$ . The anharmonicity increases the initial phonon energy. The spin–phonon interaction including quadratic and cubic terms plays an important role at low temperatures. Near and above  $T_C$  the anharmonic phonon–phonon interaction predominates.

## 5. Numerical results and discussion

We turn in this paper to the influence of the spin–phonon interaction, temperature and film thickness on the dynamical behaviour of thin films. Thin films are of particular interest because their critical properties are more susceptible to surface parameters than thicker films. In this section we shall present the numerical calculations of our theoretical results taking parameters appropriate for KDP [19]:  $J_b = 344 \text{ cm}^{-1}$ ,  $\Omega_b = 8.6 \text{ cm}^{-1}$ ,  $A_b = -5.3 \text{ cm}^{-1}$ ,  $B_b = 2 \text{ cm}^{-1}$ ,  $F_b = 28 \text{ cm}^{-1}$ ,  $R_b = -17 \text{ cm}^{-1}$ ,  $J_s = 0.2J_b$ ,  $\Omega_s = 2\Omega_b$ ,  $A_s = 2A_b$ ,  $B_s = 2B_b$ ,  $F_s = 0.2F_b$ ,  $R_s = 2R_b$ ,  $T_C = 123 \text{ K}$ . At a solid surface, the crystal symmetry is broken, and the anharmonicity is expected to be a factor of 2–3 greater than in the bulk [20, 21]. Therefore we have chosen greater surface anharmonic constants compared to the bulk. It will be shown that the enhanced surface anharmonicity leads to a decrease in energy and increase in width of a surface phonon.

### 5.1. The spin-wave spectrum

The soft mode frequencies and the damping were determined taking into account spin–phonon interactions from equation (8), by solving  $|H(E)| = 0$  (13). The temperature dependence of the soft mode frequencies is plotted in figure 1 for a simple cubic (sc) FE film for  $\mathbf{k}_{\parallel} = 0$  and different thickness of the film ( $N = 8$  and 30 layers). It is found that there are several differences between the thin films and the bulk behaviour and between the quantities with and without spin–phonon interaction. With decreasing of the film thickness the frequency decreases, too. Furthermore, the spin–phonon interaction decreases the soft-mode energies. We obtain that for  $N < 30$  layers the following expression is valid:

$$\epsilon_{\text{TF}} < \epsilon_{\text{B}}. \quad (19)$$

The soft mode of the film with  $N > 30$  layers coincides with that for the bulk.

The damping of the soft mode frequencies is plotted in figure 2 as a function of temperature with and without spin–phonon interaction for various film thickness ( $N = 8$  and 30 layers). First we consider the zero-temperature limit  $T = 0$ ,

$$\begin{aligned} \gamma_n^{\text{sp}}(T = 0) = & \frac{\pi \sin^2 \theta_n}{4} F_n^2(\mathbf{k}_{\parallel}) \delta(\bar{\omega}_n(\mathbf{k}_{\parallel}) - \epsilon_n(\mathbf{k}_{\parallel})) \\ & + \frac{\pi \cos^2 \theta_n}{N} \sum_{\mathbf{q}_{\parallel}} F_n^2(\mathbf{q}_{\parallel}) \delta(\bar{\omega}_n(\mathbf{q}_{\parallel}) + \epsilon_n(\mathbf{k}_{\parallel} - \mathbf{q}_{\parallel}) - \epsilon_n(\mathbf{k}_{\parallel})). \end{aligned} \quad (20)$$

The term proportional to  $\delta(\bar{\omega}_n(\mathbf{q}_{\parallel}) + \epsilon_n(\mathbf{k}_{\parallel} - \mathbf{q}_{\parallel}) - \epsilon_n(\mathbf{k}_{\parallel}))$  represents the scattering of a spin wave accompanied by the emission of a phonon. The  $\delta$ -functions ensure energy and momentum conservation. The conditions for satisfying the  $\delta$ -functions are deduced from the wavevector



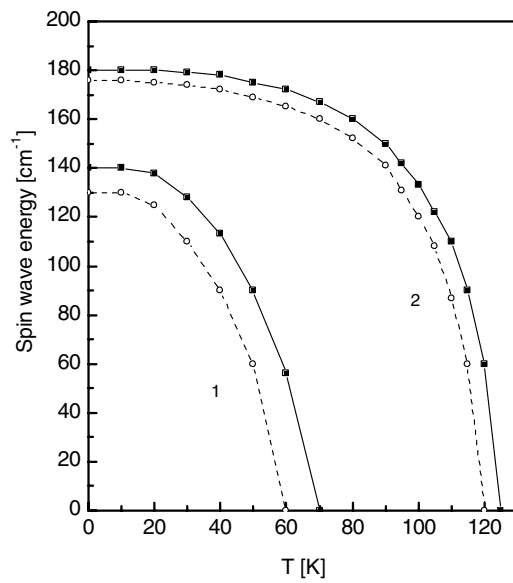


**Figure 1.** Temperature dependence of the spin-wave energy  $\epsilon$  for an sc ferroelectric film for  $J_s = 0.2J_b$ ,  $\Omega_s = \Omega_b$ ,  $B_s = 2B_b$ ,  $A_s = 2A_b$ ,  $F_s = 0.2F_b$ ,  $R_s = 2R_b$ , and different film thickness: (1)  $N = 8$ , (2) 30 layers. Dashed line, with spin-phonon interaction; full line, without spin-phonon interaction.

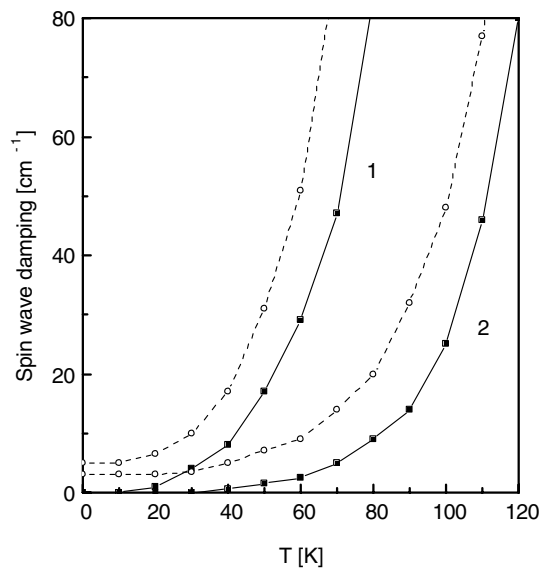


**Figure 2.** Temperature dependence of the spin-wave damping  $\Gamma_s$  for an sc ferroelectric film for the same parameters as in figure 1, and different film thickness: (1)  $N = 8$ , (2) 30 layers. Dashed line, with spin-phonon interaction; full line, without spin-phonon interaction.

dependence of the spin wave and the phonon mode. We shall be concerned with the region of small wavevector. Hence the spin waves in thin films may be damped at zero temperature due only to the spin-phonon interaction, provided the requirement due to the presence of the

$\delta$  functions in equation (20) can be satisfied. The damping due to the spin–spin interaction is zero,  $\gamma^{\text{ss}} = 0$ . Following the pseudo-spin–phonon interaction plays an important role and must be taken into account if we want to obtain correct results for the damping effects at surfaces and in thin films. The anharmonic terms do not contribute to the spin-wave damping at  $T = 0$ . At low temperatures,  $\gamma^{\text{sp}}$  is very small. With increasing temperature, the damping  $\gamma^{\text{sp}}$  increases, and the contribution of the anharmonic terms increases, too. For temperatures near  $T_C$  and above  $T_C$ , we have

$$\begin{aligned} \gamma_n^{\text{sp}}(T \geq T_C) &= \frac{\pi \sin^2 \theta_n}{4} F_n^2(\mathbf{k}_{\parallel}) \delta(\bar{\omega}_n(\mathbf{k}_{\parallel}) - \epsilon_n(\mathbf{k}_{\parallel})) \\ &+ \frac{\pi \sin^2 \theta_n}{8N} \sum_{\mathbf{q}_{\parallel}} R_n^2(\mathbf{q}_{\parallel}, \mathbf{k}_{\parallel} + \mathbf{q}_{\parallel}) (\bar{N}_n(\mathbf{q}_{\parallel}) - \bar{N}_n(\mathbf{k}_{\parallel} + \mathbf{q}_{\parallel})) \\ &\times \delta(\bar{\omega}_n(\mathbf{k}_{\parallel} + \mathbf{q}_{\parallel}) + \bar{\omega}_n(\mathbf{q}_{\parallel}) - \epsilon_n(\mathbf{k}_{\parallel})). \end{aligned} \quad (21)$$

The first term is nearly temperature independent. Hence the anharmonic terms give the main contribution to the temperature dependence of the spin-wave damping in the vicinity of  $T_C$  and above  $T_C$ ; therefore they must be taken into account.

Thinner films have larger damping. For  $N < 30$  layers we have

$$\gamma_{\text{TF}} > \gamma_{\text{B}}, \quad (22)$$

i.e.  $\gamma$  is larger for thin films than for the bulk. The spin–phonon interaction enhances the damping and contributes to the experimentally obtained line broadening. It must be taken into account in order to obtain correct results. At low temperatures the soft mode of the thin film is underdamped, whereas near  $T_C$  it is overdamped. The damping  $\gamma$  is related to the pseudo-spin-wave lifetime as  $\gamma \sim 1/\tau$ , i.e.

$$\tau_{\text{TF}} < \tau_{\text{B}}. \quad (23)$$

Thus the large damping due to the additional spin–phonon interaction indicates that the pseudo-spin-wave lifetime in thin films is less than that for the bulk, in agreement with the results of Fu *et al* [17]. The lifetime decreases with increasing spin–phonon interaction.

## 5.2. The phonon spectrum

Now we will study the effects of the spin–phonon and phonon–phonon interactions on the phonon frequency and damping in FE thin films. The phonon energy and the damping were calculated numerically using the same parameters as for the pseudo-spin-wave spectrum. Some interesting features are observed from the results obtained. The surface phonon energy  $\bar{\omega}_s$  is much smaller than the phonon energy of the inner layer  $\bar{\omega}_{N/2}$ ; the surface phonon decreases four times as much as is observed in the bulk (figure 3). This is due to the lower coordination number of the surface phonons and to the spin–phonon interaction. With increasing of the spin–phonon interaction constant the surface phonon energy decreases. The surface damping  $\Gamma_s^{\text{ph}}$  is much larger compared to the damping of the inner layer  $\Gamma_{N/2}^{\text{ph}}$ . The big difference between the surface spectrum and the spectrum of the inner layer can be explained as the result of surface modes, which are damped quickly on going into the bulk due to the confined geometry, and due to the spin–phonon interaction.

We have studied the temperature dependence of the phonon frequencies using the same model parameters as in figures 1 and 2. The phonon mode displays a nonlinear dependence on temperature when  $T$  approaches  $T_C$  (figure 4). Since it is a lattice mode this behaviour can be described to strong anharmonic effects. If we take into account only the third-order interaction terms, i.e.  $A = 0$ ,  $B = 0$ , then we obtain a linear temperature dependence close to  $T_C$  (curve 3).

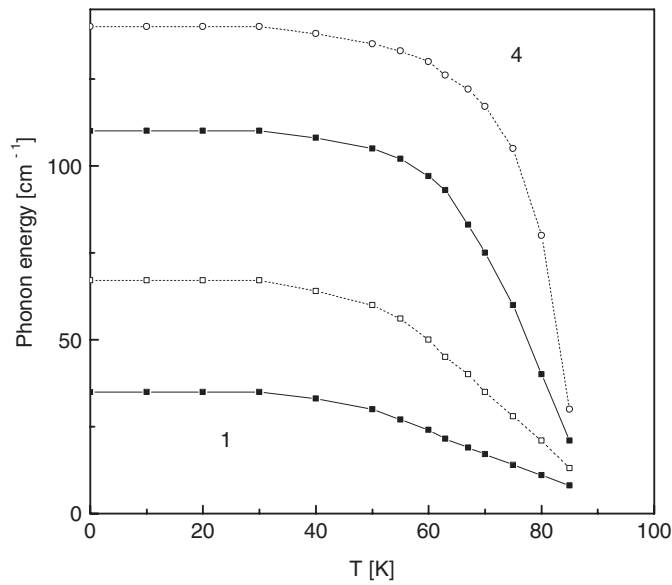


**Figure 3.** Temperature dependence of the phonon energy  $\bar{\omega}_{\text{ph}}$  for an sc ferroelectric film,  $N = 8$ , with spin–phonon interaction for the same parameters as in figure 1, and different layers.

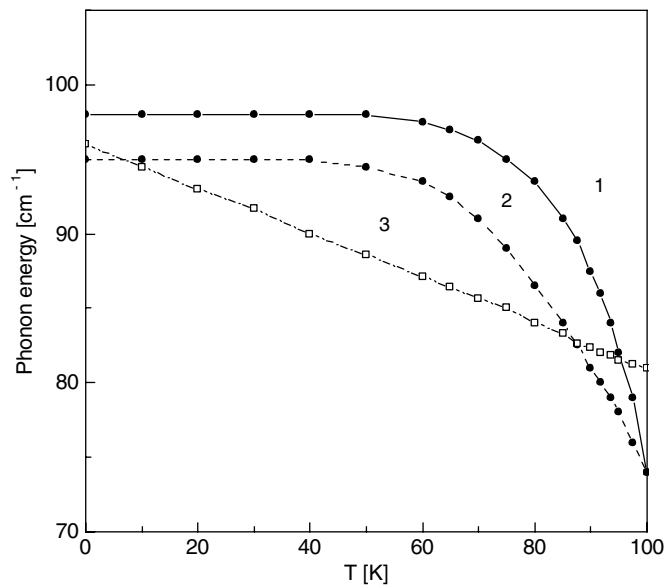


**Figure 4.** Temperature dependence of the phonon mode with  $\bar{\omega}_0 = 95 \text{ cm}^{-1}$  for an sc ferroelectric film  $N = 30$ : (1)  $\bar{\omega}_{\text{ph}}$ , (2)  $F_0 = 0, R_0 = 0$ , i.e. without spin–phonon interaction, (3)  $A_0 = 0, F_0 = 0, R_0 = 0$ , i.e. without fourth-order anharmonic phonon interaction.

It is evident that there is a strong anharmonicity affecting the phonon modes near the transition point from the ferroelectric to the paraelectric phase. The temperature dependence of the renormalized phonon energy  $\bar{\omega}$  is plotted in figure 5 for an sc FE film for different thickness of the film ( $N = 8$  and 30 layers) with and without spin–phonon interaction. It can be seen

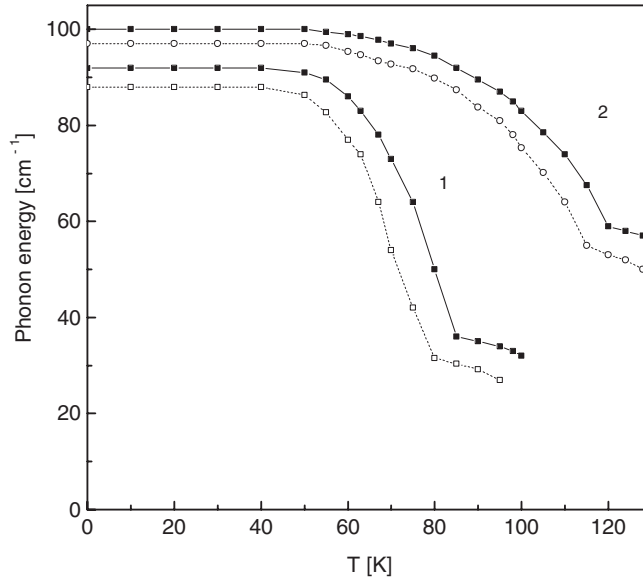


**Figure 5.** Temperature dependence of the phonon energy  $\bar{\omega}_{\text{ph}}$  for an sc ferroelectric film for the same parameters as in figure 1, and different film thickness: (1)  $N = 8$ , (2) 30 layers. Dashed line, with spin–phonon interaction; full line, without spin–phonon interaction.

that the spin–phonon interaction reduces the phonon energy and must be taken into account if we want to obtain correct results and to explain the experimental data. With increasing of the film thickness the frequency increases, too. For  $N < 30$  layers we obtain that

$$\bar{\omega}_{\text{TF}} < \bar{\omega}_{\text{B}}, \quad (24)$$

i.e. the phonon frequency of the thin film shifts to lower energy due to the existence of a surface mode and due to spin–phonon coupling. This is in agreement with the experimental data of Ishikawa *et al* [18]. The phonon energy of the film with  $N > 30$  layers coincides with that for the bulk.

Analogously to section 5.1, we want to discuss the phonon damping dependence on temperature, anharmonicity and film thickness. The temperature dependence of  $\Gamma^{\text{ph}}$  for  $N = 8$  layers obtained using the same model parameters as in figure 4 is shown in figure 6. First we consider the zero-temperature limit  $T = 0$ :

$$\begin{aligned} \Gamma_n^{\text{ph}}(T = 0) = & \frac{\pi \sigma_n \sin^2 \theta_n}{4} \left( F_n^2(\mathbf{k}_{\parallel}) \delta(\epsilon_n(\mathbf{k}_{\parallel}) - \bar{\omega}_n(\mathbf{k}_{\parallel})) \right. \\ & \left. + \frac{1}{N'} \sum_{\mathbf{q}_{\parallel}} R_n^2(\mathbf{k}_{\parallel}, \mathbf{q}_{\parallel}) \delta(\bar{\omega}_n(\mathbf{q}_{\parallel}) + \epsilon_n(\mathbf{k}_{\parallel} - \mathbf{q}_{\parallel}) - \bar{\omega}_n(\mathbf{k}_{\parallel})) \right). \end{aligned} \quad (25)$$

The term proportional to  $\delta(\bar{\omega}_n(\mathbf{q}_{\parallel}) + \epsilon_n(\mathbf{k}_{\parallel} - \mathbf{q}_{\parallel}) - \bar{\omega}_n(\mathbf{k}_{\parallel}))$  represents the scattering of a phonon accompanied by the emission of a spin wave. The  $\delta$ -functions ensure energy and momentum conservation. The conditions for satisfying the  $\delta$ -functions are deduced from the wavevector dependence of the spin wave and the phonon mode. We shall be concerned with the region of small wavevector. We get a phonon damping at  $T = 0$  due only to the pseudo-spin–phonon coupling. The phonon–phonon interaction does not contribute to  $\Gamma^{\text{ph}}$  at  $T = 0$  and at low temperatures. Following the pseudo-spin–phonon interaction plays an important role and must be taken into account if we want to obtain correct results for the damping effects

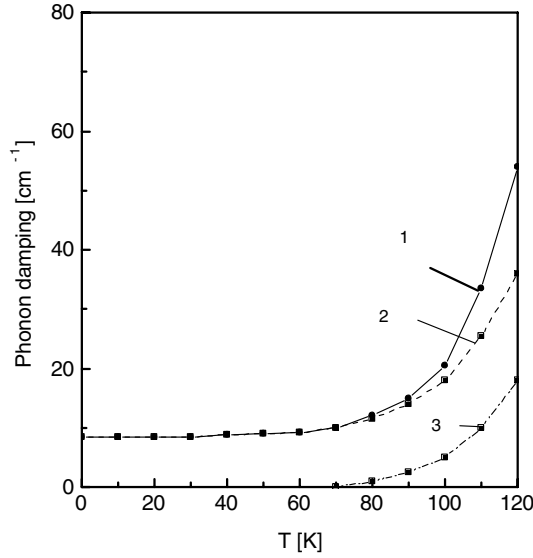


**Figure 6.** Temperature dependence of the phonon damping  $\gamma_{\text{ph}}$  with  $\bar{\omega}_0 = 95 \text{ cm}^{-1}$ : (1)  $\gamma_{\text{ph}}$ , (2)  $F_0 = 0, R_0 = 0$ , i.e. without spin–phonon interaction, (3)  $A_0 = 0, B_0 = 0$ , i.e. without phonon–phonon interaction.

at surfaces and in thin films. With increasing temperature  $\Gamma^{\text{ph}}$  increases and at  $T = T_C$  remains finite. The phonon damping in the paraelectric region is

$$\begin{aligned} \Gamma_n^{\text{ph}} = & \frac{9\pi}{N'} \sum_{\mathbf{q}_{\parallel}} B_n^2(\mathbf{k}_{\parallel}, \mathbf{q}_{\parallel}) (\bar{N}_n(\mathbf{q}_{\parallel}) - \bar{N}_n(\mathbf{k}_{\parallel} - \mathbf{q}_{\parallel})) \\ & \times [\delta(\bar{\omega}_n(\mathbf{q}_{\parallel}) - \bar{\omega}_n(\mathbf{k}_{\parallel} - \mathbf{q}_{\parallel}) - \bar{\omega}_n(\mathbf{k}_{\parallel})) - \delta(\bar{\omega}_n(\mathbf{k}_{\parallel} - \mathbf{q}_{\parallel}) - \bar{\omega}_n(\mathbf{q}_{\parallel}) - \bar{\omega}_n(\mathbf{k}_{\parallel}))] \\ & + \frac{16\pi}{N'^2} \sum_{\mathbf{q}_{\parallel}, \mathbf{p}_{\parallel}} A_n^2(\mathbf{k}_{\parallel}, \mathbf{q}_{\parallel}, \mathbf{p}_{\parallel}) [\bar{N}_n(\mathbf{p}_{\parallel}) (1 + \bar{N}_n(\mathbf{q}_{\parallel}) + \bar{N}_n(\mathbf{p}_{\parallel} + \mathbf{k}_{\parallel} - \mathbf{q}_{\parallel})) \\ & - \bar{N}_n(\mathbf{q}_{\parallel}) \bar{N}_n(\mathbf{p}_{\parallel} + \mathbf{k}_{\parallel} - \mathbf{q}_{\parallel})] \\ & \times \delta(\bar{\omega}_n(\mathbf{q}_{\parallel}) + \bar{\omega}_n(\mathbf{p}_{\parallel} + \mathbf{k}_{\parallel} - \mathbf{q}_{\parallel}) - \bar{\omega}_n(\mathbf{p}_{\parallel}) - \bar{\omega}_n(\mathbf{k}_{\parallel})). \end{aligned} \quad (26)$$

We can see that only the phonon–phonon anharmonic terms contribute to the phonon damping near and above  $T_C$ .

The phonon damping  $\Gamma_{\text{ph}} = \Gamma_{\text{ph-ph}} + \Gamma_{\text{sp-ph}}$  is plotted in figure 7 as a function of temperature for various film thickness ( $N = 16$  and 30 layers). The main signature of the spin–phonon contribution to the lifetime broadening is the temperature dependence. The spin–phonon interaction enhances the phonon damping of the thin film. The damping increases near  $T_C$ , reaches a maximum, and then remains nearly constant. It can be seen that there are several differences between the thin films and the bulk behaviour. Thinner films have larger damping. For  $N < 30$  layers we have

$$\Gamma_{\text{TF}}^{\text{ph}} > \Gamma_{\text{B}}^{\text{ph}}, \quad (27)$$

i.e. the damping is larger for thin films than that for the bulk, in agreement with the experimental data, obtained by Ishikawa *et al* [18]. The anharmonicity at the surface is 4–5 times greater than in the bulk, so it is clear that the anharmonic terms play an important role by the lifetime broadening and must be taken into account if we want to obtain correct results for the damping effects at surfaces and in thin films.

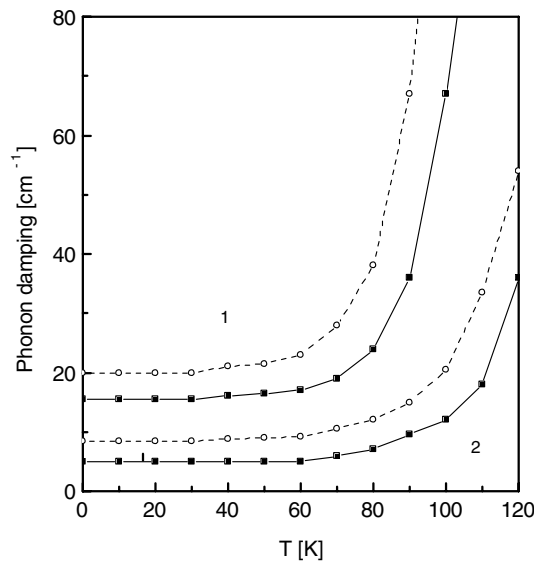


**Figure 7.** Temperature dependence of the phonon damping  $\gamma_{\text{ph}}$  for an sc ferroelectric film for the same parameters as in figure 1, and different film thickness: (1)  $N = 16$ , (2) 30 layers. Dashed line, with spin–phonon interaction; full line, without spin–phonon interaction.

## 6. Conclusions

Beyond the random phase approximation we get the renormalized pseudo-spin-wave spectrum and phonon spectrum for an sc FE thin film. The spin–phonon coupling plays an important role. It decreases the spin-wave energy of the film. The spin-wave damping is obtained and calculated numerically, too. The spin-wave damping in thin films is greater compared to the bulk case due to surface effects and anharmonic spin–phonon interactions.

We show for the first time the importance and the influence of the spin–phonon interaction on the phonon spectrum of thin FE films. The obtained temperature dependences of the phonon frequencies and the damping (figures 3 and 4) (the damping is related to the width of the half-maximum for the Raman scattering lines) taking into account anharmonic spin–phonon and phonon–phonon interaction could explain the experimental results of Raman scattering from FE thin films [14, 16–18]:

- (a) the Raman frequencies for the thin film shift remarkably to low frequencies compared with those for the bulk;
- (b) the Raman lines of the thin film are broader in comparison with those for the bulk;
- (c) the line shapes of the film become broad as the temperature approaches  $T_C$ .

## References

- [1] Scott J F, Duiker H M, Belae P D, Pouligny B, Dimmler K, Darris M, Butler D and Eaton S 1988 *Physica B* **150** 160
- [2] Binder K 1987 *Ferroelectrics* **35** 99
- [3] Tilley D R and Zeks B 1984 *Solid State Commun.* **49** 823
- [4] Cottam M G, Tilley D R and Zeks B 1984 *J. Phys. C: Solid State Phys.* **17** 1793
- [5] Wang Y G, Zhong W L and Zhang P L 1996 *Phys. Rev. B* **53** 11439

- 
- [6] Wang C L, Zhong W L and Zhang P L 1992 *J. Phys.: Condens. Matter* **3** 4743
  - [7] Sy H K 1993 *J. Phys.: Condens. Matter* **5** 1213
  - [8] Wang C L, Smith S R P and Tilley D R 1994 *J. Phys.: Condens. Matter* **6** 9633
  - [9] Wang X G, Pan S H and Yang G Z 1999 *J. Phys.: Condens. Matter* **11** 6581
  - [10] Wesselinowa J M 2001 *Phys. Status Solidi b* **223** 737
  - [11] Wang C L and Smith S R P 1996 *J. Phys.: Condens. Matter* **8** 3075
  - [12] Wesselinowa J M 2002 *Phys. Status Solidi b* **231** 187
  - [13] Feng Z C, Kwak B S, Erbil A and Boatner L A 1993 *Appl. Phys. Lett.* **62** 349
  - [14] Ching-Prado E, Reyes-Figueroa A, Katiyar R S, Majumder S B and Agrawal D C 1995 *J. Appl. Phys.* **78** 1920
  - [15] Sun L, Chen Y F, He L, Ge C Z, Ding D S, Yu T, Zhang M S and Ming N B 1997 *Phys. Rev. B* **55** 12218
  - [16] Taguchi I, Pignolet A, Wang L, Proctor M, Levy F and Schmid P E 1993 *J. Appl. Phys.* **73** 394
  - [17] Fu D S, Iwazaki H, Suzuki H and Ishikawa K 2000 *J. Phys.: Condens. Matter* **12** 399
  - [18] Ishikawa K, Yoshikawa K and Okada N 1988 *Phys. Rev. B* **37** 5852
  - [19] Wesselinowa J M, Apostolov A T and Filipova A 1994 *Phys. Rev. B* **50** 5899
  - [20] Ma S K S, de Wette F W and Alldredge G P 1978 *Surf. Sci.* **78** 598
  - [21] Jayanthi C S and Tosatti E 1985 *Phys. Rev. B* **31** 3456
  - [22] Tserkovnikov Yu 1971 *Theor. Math. Phys.* **7** 250